GPU Acceleration of the Material Point Method

Fabian Meyer

FIFTY2 Technology GmbH, 25 September 2019

GPGPU for performance enthusiasts

Why would('nt) you?

Drawbacks:

- Interactivity much easier on CPU, but slow PCI-Bus communication
- Code is mostly written against GPU architecture
- A lot of strain on the programmer

Benefits:

- Data is already on the GPU for rendering
- **Higher parallelization acceleration**

A Brief MPM Overview: Do You Want to Build a Snowman?

A short historical summary of MPM:

- Belongs to family of particle-in-cell(PIC) techniques [EHB57].
- Initial application to solids [SZS95] → MPM
- From research to production in *Disney's* animation film *Frozen* [Sto+13].
- Avalanche research [Gau+18]

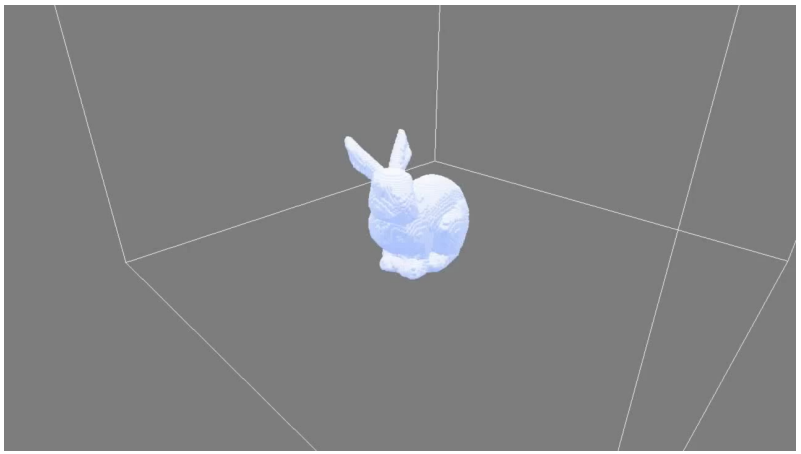

Video result of my bachelor thesis on the simulation of snow [Mey15].

PIC ideas:

- Particles store all information
- Eulerian grid as a non-deformable scratchpad

$\Rightarrow$ **meshfree**

Typical PIC/MPM roundtrip:

1. Transfer particle quantities to the grid (*P2G*)
2. Solve discretized governing equations on grid
3. Transfer back (*G2P*)

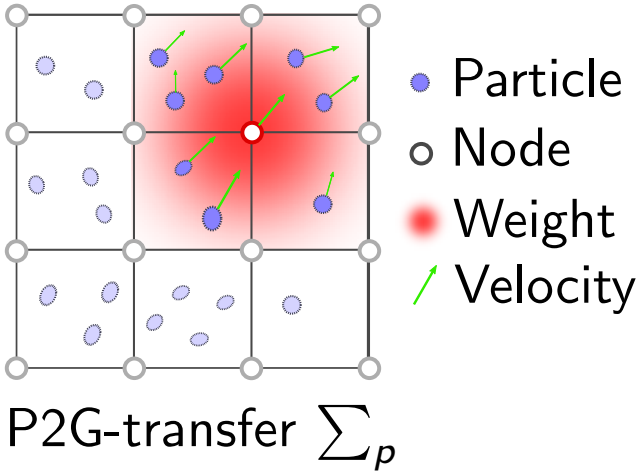

P2G-transfer $\sum_p$

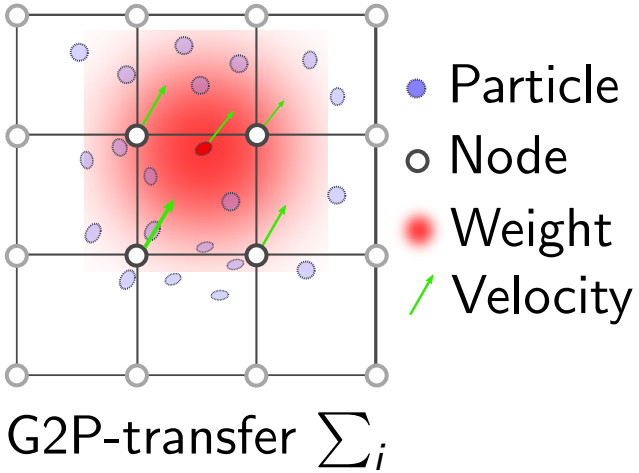

G2P-transfer $\sum_i$

Governing Equations: Conservation of Mass & Momentum

Conservation of mass, continuum assumption holds.
Lagrangian (moving with a particle ${}_0\boldsymbol{x}$):

$$ {}^t_0 J \rho({}_0\boldsymbol{x}, t) = \rho({}_0\boldsymbol{x}, 0). \tag{1} $$

Eulerian (outside observer ${}_t\boldsymbol{x}$):

$$ \frac{\partial}{\partial t}\rho({}_t\boldsymbol{x}, t) = -\vec{\nabla} \cdot (\rho({}_t\boldsymbol{x}, t)\boldsymbol{v}({}_t\boldsymbol{x}, t)). \tag{2} $$

Lagrangian and Eulerian view measure differently but give same results. Equations are given in the strong form! [Jia+16][Abe12]

Conservation of momentum:
Lagrangian (moving with a particle ${}_0\boldsymbol{x}$):

$$\rho({}_0\boldsymbol{x}, 0)\boldsymbol{a}({}_0\boldsymbol{x}, t) = \vec{\nabla} \cdot \boldsymbol{P}({}_0\boldsymbol{x}, t) + \boldsymbol{f}^{\text{body}}({}_0\boldsymbol{x}, t){}_0^t J. \tag{3}$$

Eulerian (outside observer ${}_t\boldsymbol{x}$):

$$\rho({}_t\boldsymbol{x}, t)\boldsymbol{a}({}_t\boldsymbol{x}, t) = \vec{\nabla} \cdot \boldsymbol{\sigma}({}_t\boldsymbol{x}, t) + \boldsymbol{f}^{\text{body}}({}_t\boldsymbol{x}, t) \tag{4}$$

Solving this equation will tell us how the velocity fields $\boldsymbol{v}({}_t\boldsymbol{x}), \boldsymbol{v}({}_0\boldsymbol{x})$ change on the whole domain due to acceleration $\boldsymbol{a}$.
This is important to advect particles accounting for all forces.
[Jia+16][Abe12]

Discretization of Space and Time

Space Discretization is done in a Galerkin/FEM fashion with grid based interpolants w_i. Here dyadic products of cubic b-splines suffice. w_i should satisfy at least [Gao+17]:

- Partition of unity: $\sum_i w(\boldsymbol{x} - \boldsymbol{x}_i^n) = 1$
- Identity relation: $\sum_i \boldsymbol{x}_i w(\boldsymbol{x} - \boldsymbol{x}_i^n) = \boldsymbol{x}$ $(\boldsymbol{x} = \boldsymbol{x}_p)$
- Non-negativity: $w \geq 0$.
- Limited support.
- C^1-continuity.

Shortening $w_{ip}^n = w(\boldsymbol{x}_p^n - \boldsymbol{x}_i^n)$.

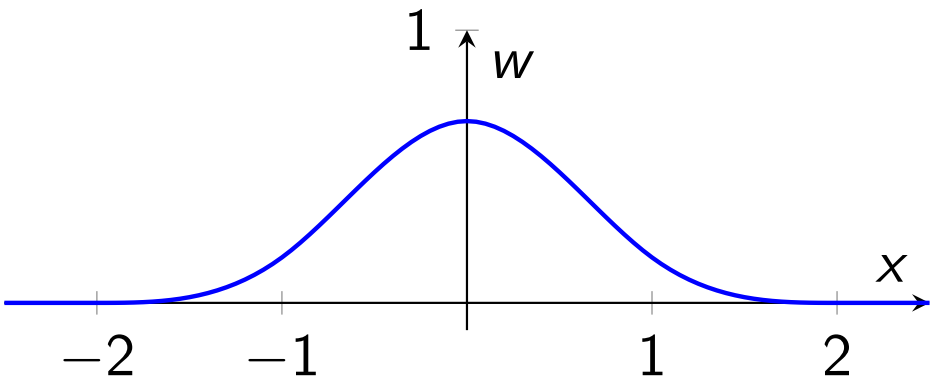

Transfer quantities from particles to grid. Numerical integration where the particles function as quadrature points [SKB08]:

$$m_i = \int_\Omega \rho(\boldsymbol{x}) w_i(\boldsymbol{x}) d\Omega \approx \sum_p \rho_p w_{ip} V_p \approx \sum_p m_p w_{ip}$$

$$A_i = \int_\Omega A(\boldsymbol{x}) w_i(\boldsymbol{x}) d\Omega \approx \sum_p A_p w_{ip} V_p.$$

APIC-transfers add a local velocity field $\boldsymbol{C}_p$ around $\boldsymbol{v}_p$:

$(m\boldsymbol{v})_i = \sum_p w_{ip} m_p \left(\boldsymbol{v}_p + \boldsymbol{C}_p(\boldsymbol{x}_i - \boldsymbol{x}_p)\right)$

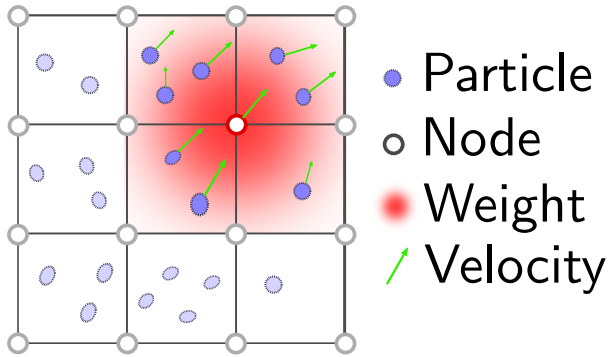

P2G-transfer $\sum_p$

The MPM can be described in the weak formulation (FEM: virtual quantities). This allows us to 'shift' the derivative:

- $\boldsymbol{A}_p = \sum_i \boldsymbol{A}_i w_{ip}$
- $\nabla \boldsymbol{A}_p = \sum_i \boldsymbol{A}_i \nabla w_{ip}^T$
- $\nabla \cdot \boldsymbol{A}_p = \sum_i \boldsymbol{A}_i^T \nabla w_{ip}$

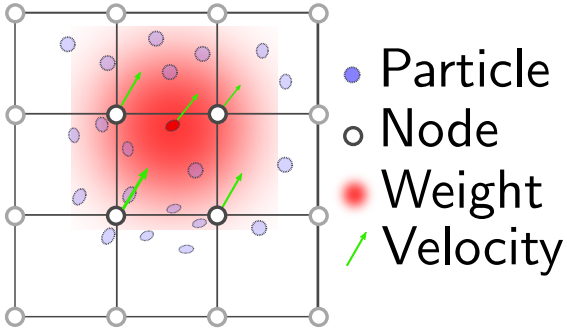

G2P-transfer $\sum_i$

Time discretization with implicit midpoint scheme:

$$v_i^{n+1} - v_i^n = \frac{\Delta t}{m_i^n} f_i^{n+\frac{1}{2}} = \frac{\Delta t}{m_i^n} f\left(t^n + \frac{\Delta t}{2}, \frac{1}{2} y^n + \frac{1}{2} y^{n+1}\right)$$

- **implicit** requires linear system solve $\Rightarrow$ more stable, larger time steps
- **midpoint** as it conserves angular momentum

Layout of the data: SoA vs. AoS

Coalescing:

SoA-Layout

```
struct Container{
  vec4 positions[n];
  vec4 velocities[n];
} Particles;
```

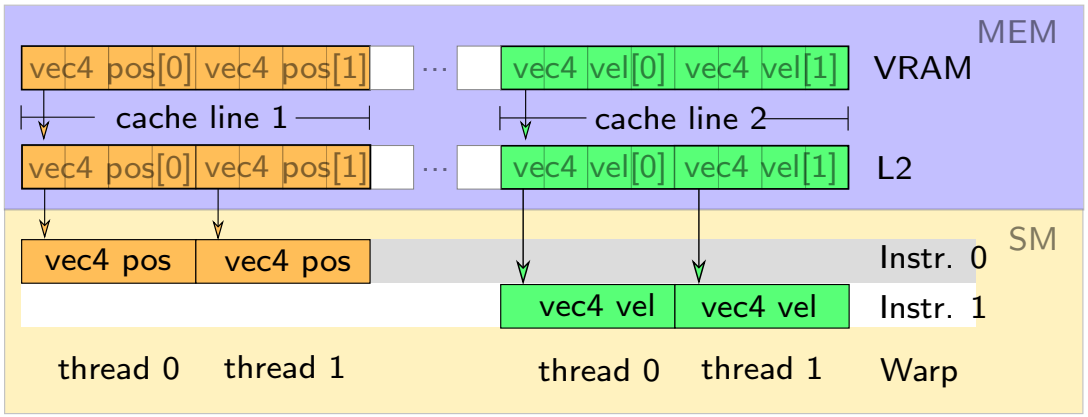

Structures of arrays(SoA)

AoS-Layout

```
struct Particle {
  vec4 position;
  vec4 velocity;
} Particles[n];
```

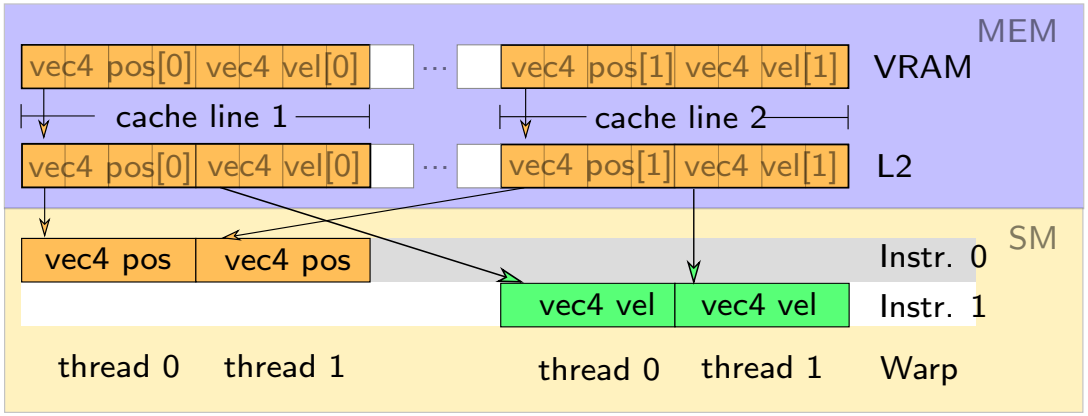

Arrays of structures(AoS)

Nvidia Nsight[NVI] now offers metrics to identify bottlenecks:

Metric	**Description**
VRAM SOL%	memory througput w.r.t. to hardware limit
SM SOL%	instruction throughput
L2 SOL%	L2-cache throughput
Tex SOL%	L1-cache throughput
SM Issue Util.%	amount of cycles an instr. was issued

A simple map(`y=length(x)`) shader on 1024×1024 Elements SoA vs. AoS differences:

Layout	$\Delta t_c(\mu s)$	Speedup	VRAM	SM	L2	SM Issue Util.
AoS(1 instr.)	243	-	77.7%	7.3%	30.3%	6.8%
SoA(1 instr.)	**120**	2.26x	75.4%	**14.3%**	29.4%	**14.0%**
AoS(2 instr.)	275	-	61.3%	**41.8%**	**53.8%**	48.9%
SoA(2 instr.)	240	1.16x	75.4%	29.4%	20.0%	62.3%

⇒ SoA increases coalescing for non-random access.

Parallel Reduction & Scan

Assuming an associative `binary_op(x,y)`$:= x \circ y$, a neutral element e of the `binary_op`, and an array of values $[a_0, a_1, ..., a_n]$.

- **Parallel reduction** computes the value:

$$r = a_0 \circ a_1 \circ ... \circ a_n. \tag{5}$$

- (Exclusive) **scan** computes the array:

$$[e, a_0, (a_0 \circ a_1), (a_0 \circ a_1 \circ a_2), \ ... \ , (a_0 \circ a_1 \circ a_2 \circ ... \circ a_{n-1})]. \tag{6}$$

Here, only shared memory approaches without warp shuffle operations.

Shared Memory Bank Conflicts:

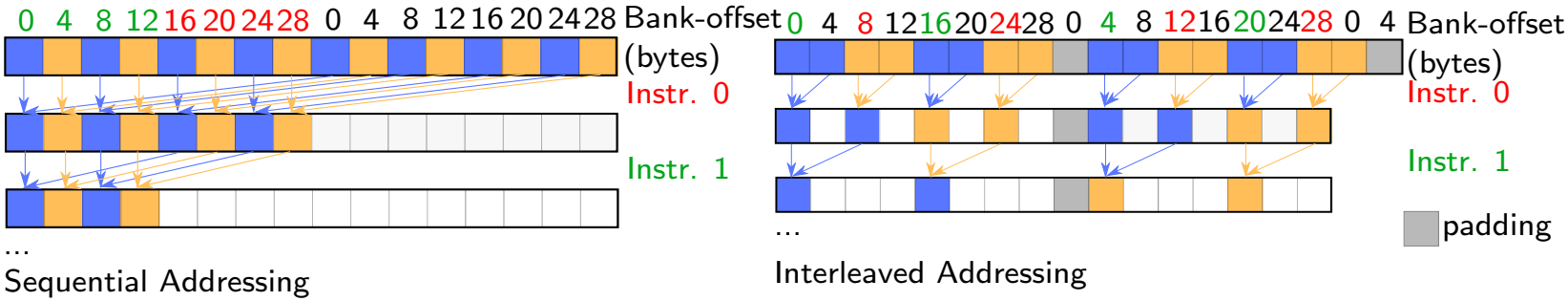

Interleaved addressing causes bank conflicts (Short Scoreboard activity) $\Rightarrow$ padding needed.

Method	Δt_c	Speedup	VRAM	SM	Sel. Warp-Stall Reas.
Interl. no padd.	305	-	23.0%	**60.9%**	S. Scoreb.(17.2%)
Sequential	141	2.16x	**49.8%**	37.1%	**S. Scoreb.(2.0%)**

Table: Parallel reduction on 1024×1024 vectors with `y=length(x)` as input.

More elements than thread group size require pyramid schemes.

Sequential work: multiple elements per thread.

- Memory latency hiding (Long Scoreboard up)
- Higher reduction factor each dispatch ⇒ Less global memory indirections
- Unrolling loops can help but adds register pressure.

Method	Δt_c	Speedup	VRAM	SM	Sel. Warp-Stall Reas.
Sequential	141	2.16x	49.8%	37.1%	S. Scoreb.(2.0%)
Seq. (2x)	100	3.05x	69.5%	26.2%	L. Scoreb.(80.1%)
Seq. (128x)	98	3.1x	**72.9%**	16.9%	**L. Scoreb.(84.4%)**
Seq. (256x)	101	3.0x	66.4%	14.6%	L. Scoreb.(76.9%)

Table: Parallel reduction on 1024×1024 vectors with `y=length(x)` as input. Methods have 504, 8, 4 thread groups, respectively. A GTX970 has 13 SMs.

Scan is similar but cannot profit as much from sequential work having to keep multiple elements in register memory.

Binning & Counting Sort: Where Are You?

Grid node does not know its neighboring particles ⇒ Binning.

Binning combines nicely with **Counting Sort:**

1. **Binning**: Per node counting.
2. **Scan**: Computes new memory offset for particles.
3. **Reordering**: Give back indexing list or do deep copy.

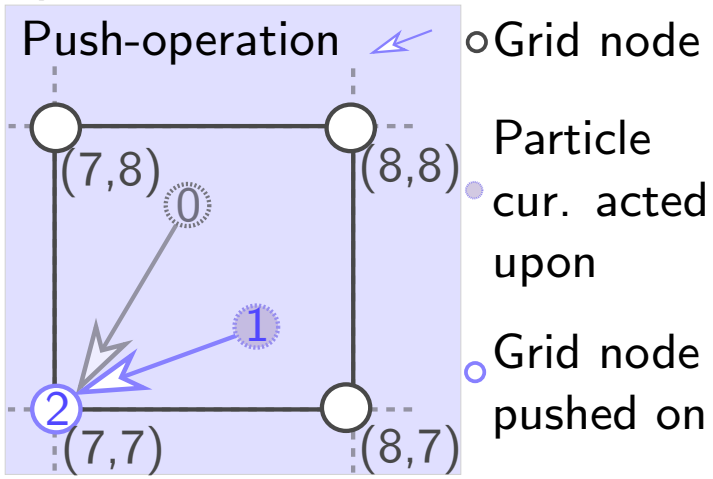

Sorting can dramatically increase workload performance of subsequent steps for neighboring queries:

1. Deep sorted accesses are now **coalesced**.
2. **Data reuse** due to L2-Cache and/or shared memory.

Double buffer particles to use last sorted state as input for new sorting to profit from item 1 and 2!

Ordering	$\Delta t_c(\mu s)$	Speedup	VRAM	SM	L2	L2-Hit
Random	1,516	-	25.0%	3.4%	9.1%	10.8%
Deep sorted	218	6.95x	**75.3%**	24.4%	**35.0%**	**37.8%**

Table: Order dependency of binning of 1024×1024 randomly positioned particles in a $128 \times 128 \times 128$ grid.

The MPM Specific Transfers

All MPM operations belong to one of those parallelization schemes:

- 1 thread : 1 particle: $\square_p = \square_p \circ \square_p \circ ... \circ \square_p$.
- 1 thread : 1 node: $\square_i = \square_i \circ \square_i \circ ... \circ \square_i$.
- G2P-transfer: $\square_p = \sum_i \square_i \circ \square_{ip}$.
- P2G-transfer: $\square_i = \sum_p \square_p \circ \square_{ip}$.

MPM-Transfers are executed **multiple times per physical frame** with varying numbers of variables and mathematical operations.

$\Rightarrow$ Preprocessing steps only need to be done **once per physical frame**. Sorting already introduced as one of these.

G2P-Transfer: $\square_p = \sum_i \square_i \circ \square_{ip}$.

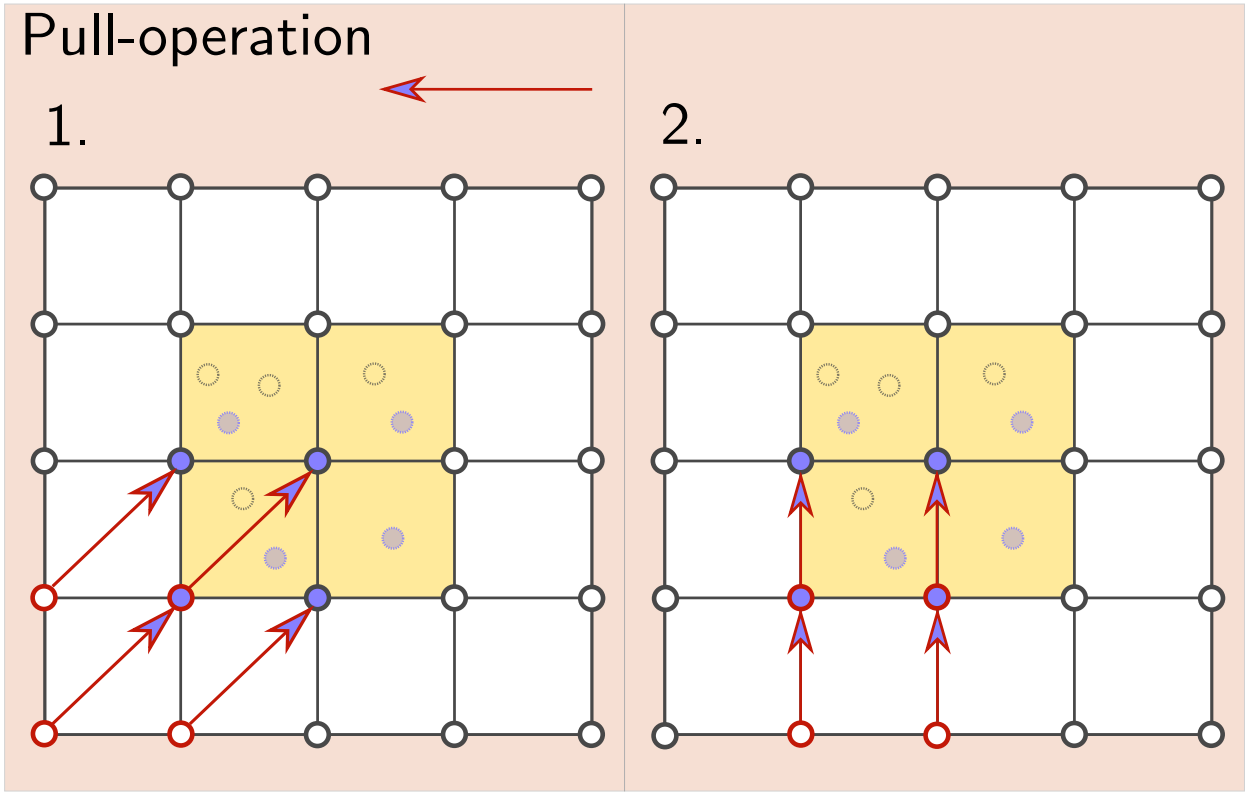

Pull-Operations read!

Similar to filter or stencil operations on the GPU:

- 1 node : 1 thread, split grid into blocks corr. to thread groups.
- Interpolation function however dependent on particle position.
- Needs to be rerun for every particle in the cell.

Typical setup of transfers:

1. Initialize shared memory (pull: with nodes from global memory).
2. Perform transfers.
3. Write back to global memory (push: global atomics since writes on halo).

P2G-transfer: $\square_i = \sum_p \square_p \circ \square_{ip}$.

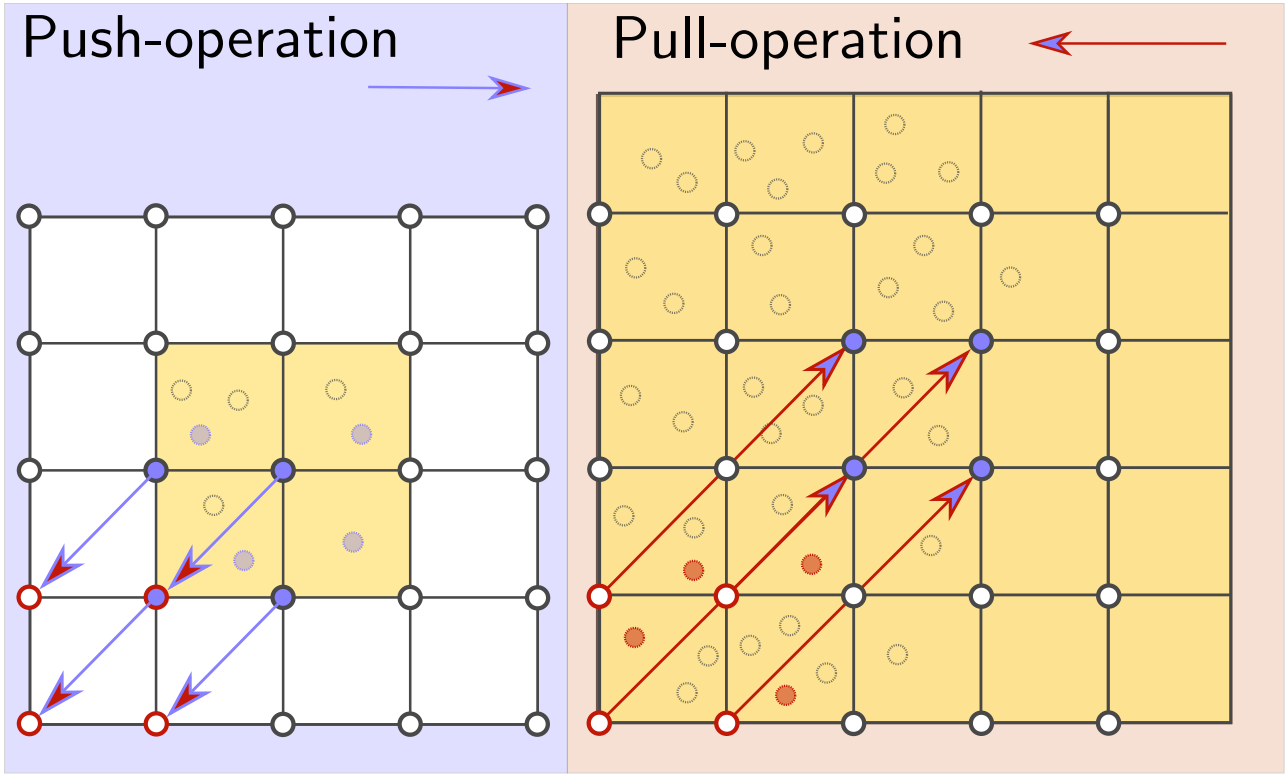

Pull-Operations read, Push-operations write!

$\Rightarrow$ Race conditions.

Typically simulation domain(grid) much bigger than simulation model. Filtering inactive blocks as a preprocess improves performance.

- Block is active if any cell counter is active.
- Cell counter is active if it has at least one particle.

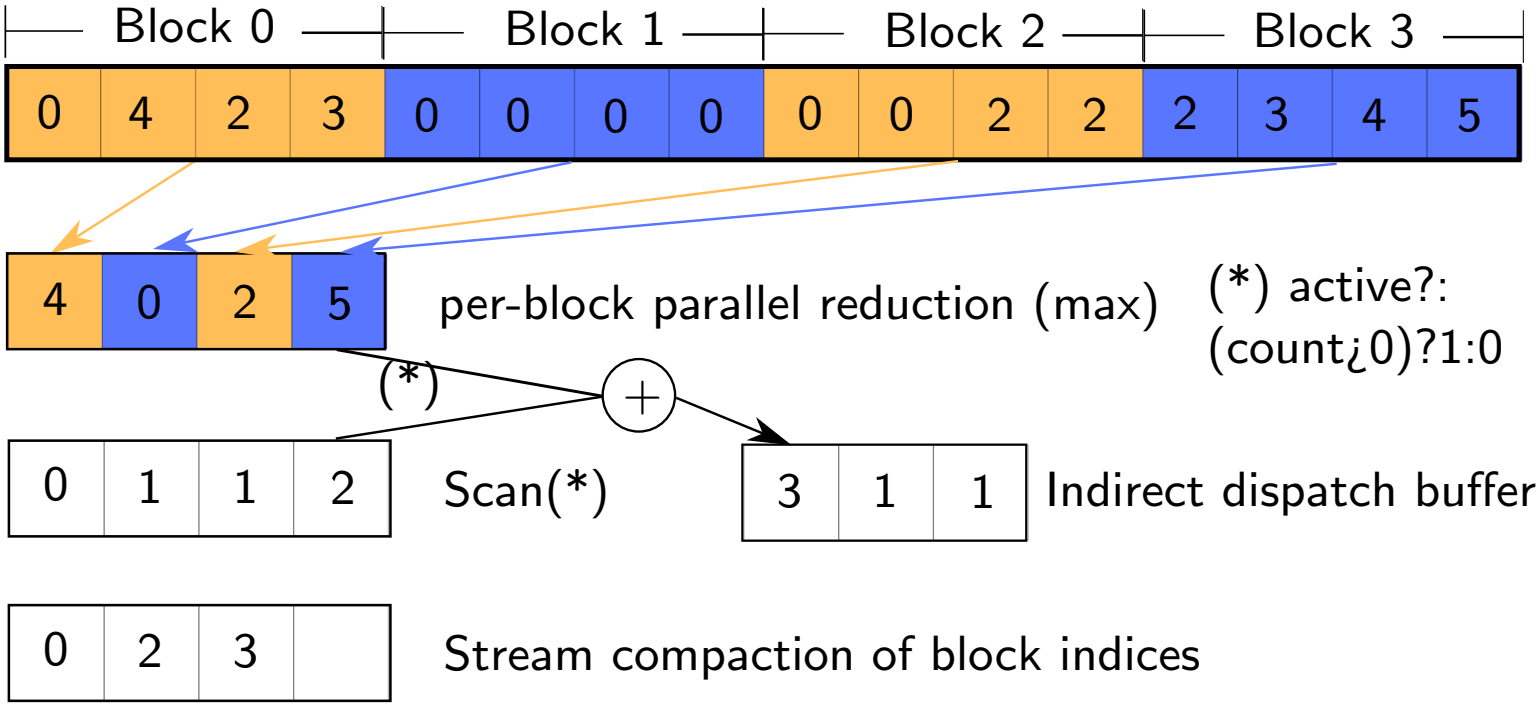

- Block and halo are always target of shared memory operations $\Rightarrow$ P2G-pull low occupancy.
- **Batching** multiple particles can increase performance due to hiding synchronization, unroll!
- Transfers respect shared memory bank conflicts fully.
- **Warp divergence** for varying cell counts.

Method	$\Delta t_c(\mu s)$	Speedup	VRAM	L2	SM
global	44,442	-	4.6 %	34.4%	7.7%
global sorted	20,484	2.21x	7.0 %	**44.0%**	16.1%
P2G-sync	**2,595**	17.47x	5.9%	7.6%	**67.0%**

P2G-transfers of one uniformly million particles with 4 particles per cell with random velocities between $v_x, v_y, v_z \in [-1.0; 1.0]$ in a $128 \times 128 \times 128$ grid. Block size is (8,4,4).

A comparison to [Gao+18]

Simultaneously being worked on. Largely same decision making:

	Me	**[Gao+18]**
Sort	Count/Histogram for each var.	Count/Histogram sel. variables
Filtering domain	Filter-op.	Sparse Grid structure
Transfers	Shared mem. only	Warp-shuffle op.

Warp shuffle allows for fast parallel segmented reduction of cells of varying counts.
$\Rightarrow$ Solves warp divergence and shared memory issues mostly, thread groups now correspond to particles. Faster for varying counts.

Thank you for your attention!

- **Bachelor thesis**: https://github.com/MeyerFabian/snow
- **Master thesis**: https://github.com/MeyerFabian/msc
- **Presentation**: https://github.com/MeyerFabian/msc/pres
- **Code** (right now): https://github.com/mpm-msc/snow

Questions?

Rohan Abeyaratne. *Volume II of Lecture Notes on,The Mechanics of Elastic Solids: Continuum Mechanics*. http://web.mit.edu/abeyaratne/Volumes/RCA_Vol_II.pdf. [Online; accessed 08-November-2018]. MIT Department of Mechanical Engineering, 2012.

Klaus-Jürgen Bathe. *Finite element procedures*. Klaus-Jurgen Bathe, 2006.

Martha W Evans, Francis H Harlow, and Eleazer Bromberg. *The particle-in-cell method for hydrodynamic calculations*. Tech. rep. LOS ALAMOS NATIONAL LAB NM, 1957.

Ming Gao et al. "An adaptive generalized interpolation material point method for simulating elastoplastic

materials". In: *ACM Transactions on Graphics (TOG)* 36.6 (2017), p. 223.


Ming Gao et al. "GPU Optimization of Material Point Methods". In: *ACM Trans. Graph.* 37.6 (2018), 254:1–254:12. ISSN: 0730-0301.


Johan Gaume et al. "Unified modeling of the release and flow of snow avalanches using the Material Point Method". In: Aug. 2018.


Chenfanfu Jiang et al. "The material point method for simulating continuum materials". In: *ACM SIGGRAPH 2016 Courses*. ACM. 2016, p. 24.


Fabian Meyer. "Simulation von Schnee". Bachelor's Thesis. Universität Koblenz-Landau, Institut für Computervisualistik, 2015.


NVIDIA Corporation. *NVIDIA Nsight*. https://docs.nvidia.com/nsight-visual-studio-edition/Content/Performance_Markers_OGL.htm. [Online; accessed 5-December-2018].


Michael Steffen, Robert M Kirby, and Martin Berzins. "Analysis and reduction of quadrature errors in the material point method (MPM)". In: *International journal for numerical methods in engineering* 76.6 (2008), pp. 922–948.


Alexey Stomakhin et al. "A material point method for snow simulation". In: *ACM Transactions on Graphics (TOG)* 32.4 (2013), p. 102.


Deborah Sulsky, Shi-Jian Zhou, and Howard L Schreyer. "Application of a particle-in-cell

method to solid mechanics". In: *Computer physics communications* 87.1-2 (1995), pp. 236–252.

The Pretty Strong but Mathematically Weak Formulation

Weak Formulation (or Principle of Virtual Work):
Dot product equations with arbitrarily 'test functions' $\boldsymbol{q}$ and apply divergence theorem:

$$\int_{\Omega^0} {}_0\boldsymbol{q} \cdot \left[({}_0\rho_0)({}_0\boldsymbol{a}) - {}_0\boldsymbol{f}^{\text{body}\,t}_{\;0}J \right] d_0\boldsymbol{x} = \int_{\partial\Omega^{t^n}} {}_t\boldsymbol{q} \cdot \boldsymbol{\sigma}\, d_t\boldsymbol{A} - \int_{\Omega^{t^n}} \nabla_t \boldsymbol{q} : \boldsymbol{\sigma}\, d_t\boldsymbol{x}. \quad (7)$$

A strong solution is also a solution to the weak formulation. Leave out body forces(like gravity) and boundary condition (e.g. collisions) for now:

$$\int_{\Omega^0} {}_0\boldsymbol{q} \cdot ({}_0\rho_0)({}_0\boldsymbol{a}) d_0\boldsymbol{x} = \int_{\Omega^{t^n}} \nabla_t \boldsymbol{q} : \boldsymbol{\sigma}\, d_t\boldsymbol{x}. \quad (8)$$

Weak Derivative:

$y = |t|$ has weak derivative:

$$v = \begin{cases} -1, & \text{if } t < 0 \\ c, & \text{if } t = 0 \\ 1, & \text{if } t > 0 \end{cases}$$

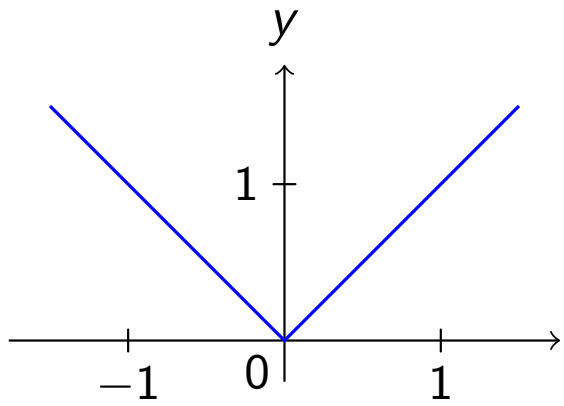

Heaviside step function has no weak derivate:

$$s = \begin{cases} 0, & \text{if } t < 0 \\ 1, & \text{if } t \geq 0 \end{cases}$$

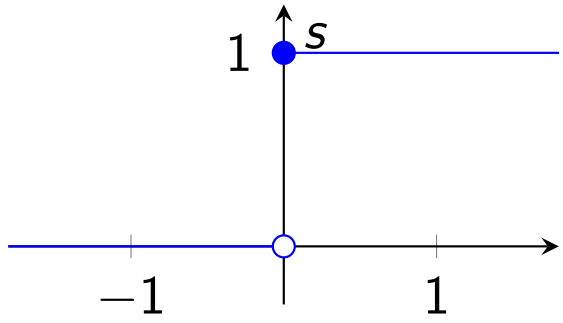

Allows for point loads, material discontinuities and more. [Bat06]

Space Discretization is done in a Galerkin/FEM fashion with grid based interpolants w_i with limited support. Here dyadic products

$$w_i(\boldsymbol{x}) = w(\boldsymbol{x} - \boldsymbol{x}_i) = w(\frac{1}{h}(x - x_i))w(\frac{1}{h}(y - y_i)w(\frac{1}{h}(z - z_i)) \quad (9)$$

of cubic b-splines suffice:

$$w(x) = \begin{cases} \frac{1}{2}|x|^3 - |x|^2 + \frac{2}{3} & 0 \leqslant |x| < 1 \\ \frac{1}{6}(2 - |x|)^3 & 1 \leqslant |x| < 2 \\ 0 & 2 \leqslant |x| \end{cases} . \quad (10)$$